Construction and Building Materials 159 (2018) 408–416

Contents lists available at ScienceDirect

Construction and Building Materials

journal homepage: www.elsevier.com/locate/conbuildmat

Kernel machines and firefly algorithm based dynamic modulus prediction model for asphalt mixes considering aggregate morphology

Dharamveer Singh [a,*], Saurabh Maheshwari [a], Musharraf Zaman [b], Sesh Commuri [c]

[a] Civil Engineering Department, Indian Institute of Technology Bombay, Powai, Mumbai 400076, India
[b] The University of Oklahoma, Norman, OK 73019, USA
[c] Department of Electrical and Biomedical Engineering, University of Nevada, Reno, USA

HIGHLIGHTS

- SVR proved successful in outperforming Witczak and ANN models for estimation of dynamic modulus of asphalt mixes.
- Aggregate shape parameters are considered in estimation of dynamic modulus.
- An approach for formulation of SVR-FA model equations for direct prediction of HMA stiffness is also discussed.
- SVR-FA algorithm is capable of successfully predicting dynamic modulus values using the aggregate shape parameters.

ARTICLE INFO

Article history:
Received 26 June 2017
Received in revised form 15 September 2017
Accepted 31 October 2017

Keywords:
Dynamic modulus
Support vector regression
Firefly algorithm
Cumulative shape index factor

ABSTRACT

Artificial Intelligence algorithm support vector regression (SVR) has proved successful in outperforming conventional Witczak and ANN models for estimation of dynamic modulus (E^*) of asphalt mixes. However, there were two issues related to the development of E^* prediction models that the present study addresses. Firstly, since aggregates occupy almost 95% by weight of HMA, it is quite possible that the morphology of these aggregates play an important role in influencing the E^* values. To address this issue, aggregate shape parameters, namely, angularity, sphericity, texture and form were used with aggregate gradation for stiffness estimation. Secondly, to fine tune the hyper-parameters firefly algorithm (FA) was coupled with SVR. E^* tests of 20 HMA mixes having different sources, sizes of aggregates, and volumetric properties were conducted at 4 temperatures and 6 frequencies. Aggregate shape parameters were measured using the automated aggregate image measurement system (AIMS). SVR-FA models were developed that predicted the E^* with an R^2 of 0.98. SVR-FA models were compared with SVR and ANN models for E^* prediction. Further, a sensitivity analysis was conducted to identify the important input parameters. Lastly, an approach for formulation of SVR-FA model equations for direct prediction of HMA stiffness is also discussed. FA proved instrumental in improving the efficiency of SVR by optimizing the hyper-parameters with lesser manual effort. Finally, it was concluded that SVR-FA algorithm is capable of successfully predicting the E^* values using the aggregate shape parameters.

1. Introduction

Dynamic Modulus (E^*) is a fundamental property of asphalt mixes that has a significant effect on the major pavement distresses such as, fatigue, rutting, and low temperature cracking [1]. Also, as per the Mechanical Empirical Pavement Design Guide [2], E^* is an important parameter required for the calculation of damage accumulation over the life cycle of a flexible pavement. E^* of a mix can be directly measured through laboratory tests prescribed by AASHTO TP62-06 [3]. However, the laboratory tests can be expensive, time-consuming and depend on the sensitivity of the instrument [4]. Hence, to simplify the situation many researchers used predictive models namely, Witczak models [5,6], Al-Khateeb model [7] and Hirsch model [8] to estimate E^*, based on aggregate gradation, volumetric properties of compacted mix and asphalt binder properties. Due to the regression relationship between E^* and independent variables, prediction accuracy of these models vary with the test temperature, type of mix and aggregate gradation [9–12]. To enhance the prediction capability of the models,

* Corresponding author.
E-mail addresses: dvsingh@iitb.ac.in (D. Singh), saurabhmaheshwari52@gmail.com (S. Maheshwari), zaman@ou.edu (M. Zaman), scommuri@unr.edu (S. Commuri).

https://doi.org/10.1016/j.conbuildmat.2017.10.133
0950-0618/

Far et al. [12] and Ceylan et al. [10,11,13] developed Artificial Neural Network (ANN) models for E* prediction, which resulted in significant improvement in accuracy as compared to the multi-regression models. Recently, another efficient machine learning algorithm called Support Vector Regression (SVR) was proposed for the prediction of E* [14,15]. The results showed that SVR could outperform ANN and multi-regression models in terms of prediction accuracy.

SVR works on the principle of structural risk minimization, unlike ANN which is based on empirical risk minimization. Hence, SVR can give predictive models with greater generalization capability [16]. Also, SVR results in unique solutions unlike conventional ANN, which suffers from risk of encountering local minima. The motivation behind the application of SVR includes, (1) capability of modeling non-linear behavior using appropriate kernels, (2) ability to generalize better due to a bound on overall risk along with the minimization of training error, (3) using necessary data points known as support vectors to solve the optimization problem and (4) requirement of lesser training data. However, one of the drawbacks of using SVR is that there is no straight-forward method for optimization of its hyper-parameters. Gopalakrishnan and Kim [13] mentioned the need of further fine tuning of SVR control parameters to achieve better prediction accuracy. To address this issue, recently, researchers have explored the application of Firefly algorithm (FA) with SVR to enhance the accuracy of a prediction model and concluded that SVR-FA outperformed algorithms like ANN, SVR and genetic programming [17,18].

Although all the above approaches utilized aggregate gradations, but none of them considered aggregate shape parameters as potential input variables for E* estimation. Due to the presence of 95% of aggregate (by weight) in asphalt mixes, their shape properties, namely, angularity, sphericity, texture and form (2-D) are expected to have a direct effect on performance and serviceability [19–22]. Bari and Witczak [6] mentioned that mixes with similar volumetric properties and aggregate gradation may result in different values of E*. Therefore, it is important to emphasize the importance of aggregate shape properties in estimation of E*.

In the present study, E* tests were conducted for 20 different mixes at 4 temperatures and 6 frequencies. The aggregates of each mix were divided into different sizes of coarse and fine aggregates. Shape parameters, namely, angularity, sphericity, form and texture for these aggregates were measured using Aggregate Image Measurement System (AIMS). SVR-FA algorithm was used to develop E* predictive model using cumulative shape index factors, volumetric properties of mix, viscosity of binder and frequency. Cumulative shape factors considered the combined effect of aggregate gradation and particle morphology. FA was utilized to fine-tune the SVR hyper-parameters to enhance the accuracy of prediction. Regression coefficient, mean average relative error and overfitting ratio were calculated to evaluate the accuracy of prediction. SVR-FA model is further compared with ANN and SVR models for E* prediction. A sensitivity analysis to quantify important parameters for E* estimation was done. Lastly, an approach for formulation of model equations using SVR-FA algorithm to predict E^* directly is also discussed.

2. Objective of the study

- Development of SVR-FA models for evaluating E* using cumulative shape factor indices of aggregates.
- Comparison of the developed SVR-FA model with artificial neural networks (ANN) and support vector machine regression (SVR) models.
- Development of SVR-FA model equations for direct prediction of E*.
- Study sensitivity analysis of input parameters for estimation of E*.

3. Background on Support Vector Regression

Support Vector Machine Regression (SVR) is a machine learning algorithm based on statistical learning theory, introduced by Vapnik [23,24]. SVR aims at finding an optimal regression function that has at most ε deviation from the original targets y, and is also as flat as possible. Such a function, $f(x)$ is represented in Eq. (1).

$$f(x) = < w, x > + b; w \in X,\ b \in R \tag{1}$$

where <·,·> denotes the dot product in X. One way to ensure the flatness of the function is to minimize the norm of parameter w. Though it is required that optimal regression function always predict the targets y with a precision ε, but in reality, this may result in infeasible constraints while solving the optimization problem. Hence, to deal with this infeasibility, slack variables ξ_i^*, ξ_i (upper and lower bound on training error, respectively) are introduced. Hence, the optimization problem of SVR can be expressed as shown in Eq. (2).

$$\begin{aligned} &\bullet \ \text{minimize } 1/2 * ||w||^2 + C\sum_{i=1}^{l}(\xi_i + \xi_i^*) \\ &\bullet \ \text{subject to } \{y_i - < w, x_i > - b \leqslant \varepsilon + \xi_i \\ &\qquad \{< w, x_i > + b - y_i \leqslant \varepsilon + \xi_i^* \\ &\qquad \xi_i, \xi_i^* \geqslant 0 \end{aligned} \tag{2}$$

The hyper-parameter C in Eq. (2) is the trade-off between flatness of the function and amount up to which the deviations greater than ε are allowed [25]. Very large values of C may end up in over-penalizing the error bounds, hence can result in over-fitting. On the contrary, smaller values of C may lead to under-fitting. The hyper-parameter ε denotes the width to fit the training data. It represents the trade-off between the sparseness and closeness in the representation of the data [14]. The data points that lie outside the 'ε-tube' are dealt with the cost function shown in Eq. (3), known as ε-insensitivity loss function. Fig. 1 depicts the ε-insensitivity loss function graphically.

$$L_\varepsilon(y) := \begin{Bmatrix} 0 & if\ |\xi| \leqslant \varepsilon \\ |\xi| - \varepsilon & otherwise \end{Bmatrix} \tag{3}$$

where $|\xi| = |y - f(x)|$.

The above formulated optimization problem is solved using the Lagrange multiplier approach and the solution of the optimal regression function is expressed as Eq. (4).

$$f(x) = \sum_{i=1}^{l}((\alpha_i - \alpha_i^*) < x_i, x > + b), \quad \text{where } 0 < \alpha_i, \alpha_i^* < C \tag{4}$$

α_i, α_i^* are the Lagrangian multipliers and are equal to zero for the data set that lie within the ε-tube as per the Karush-Kuhn-Tucker (KKT) conditions. In other words, only the points that lie outside the ε-tube (i.e. the region between the dashed lines in Fig. 1) have non-zero α_i, and α_i^*, which are known as Support Vectors. Only support vectors are used to determine the optimal regression function, as only for these points α_i, α_i^* are non-zero.

In the case of non-linear relationship, instead of trying to fit a non-linear model, the training data x_i are transformed to a high dimensional space R^D by mapping φ: $R^d \rightarrow R^D$ by using kernel functions. Hence, the dot product $< x_i, x >$ in the linear space becomes $< \varphi(x_i), \varphi(x_j) >$ in the high-dimensional space. Thus, the optimal regression function for the non-linear problem is given in Eq. (5).

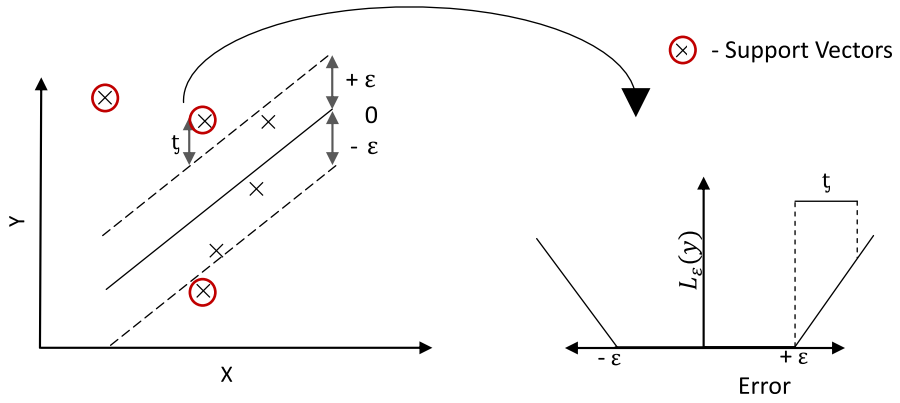

Fig. 1. ε-insensitivity loss function.

$$f(x) = \sum_{i=1}^{l}((\alpha_i - \alpha_i^*)K(x_i, x_j) + b) \tag{5}$$

Fig. 2 explains the architecture of SVR. Some of the commonly used kernel functions are linear, radial basis, polynomial and spline. The detailed theory behind SVR is explained in the study of Vapnik [23,24] and in tutorials by Smola and Scholkopf [26].

3.1. Background on firefly algorithm

FA is a metaheuristic evolutionary algorithm that is inspired by the flashing behavior of fireflies, which use their natural glowing mechanism to attract other fireflies. It was introduced by Yang [27] and is capable of finding both global and local minima of the cost function very effectively. FA can outperform genetic algorithm and particle swarm optimization in solving optimization problems [28]. There are two important issues associated with FA, i.e., variation of light intensity and formulation of attractiveness of fireflies. Attractiveness of the fireflies is determined by its brightness, which is assumed to be directly proportional to the objective function as shown in Eq. (6).

$$I(x) \propto f(x) \tag{6}$$

Brightness is assumed to vary with (1) distance r_{ij} between fireflies i and j, and (2) degree of absorption of the media. To consider the effect of both, the brightness is expressed as the Gaussian form shown in Eq. (7).

$$I = I_o e^{-\gamma r^2} \tag{7}$$

where I_o is the original light intensity. As the attractiveness of the firefly as seen by the adjacent fireflies is proportional to its brightness, hence, it can be expressed as shown in Eq. (8).

$$\beta(r) = \beta_0 e^{-\gamma r^2} \tag{8}$$

where β_0 is the attractiveness at r = 0. The distance r_{ij} between any two fireflies i and j at x_i and x_j, is calculated using Cartesian distance given by Eq. (9).

$$r_{ij} = ||x_i - x_j|| = \sqrt{\sum_{k=1}^{d}(x_{i,k} - x_{j,k})^2} \tag{9}$$

where d is the total number of fireflies. Finally, the movement of firefly i to a more attractive firefly j is calculated as per Eq. (10).

$$x_i = x_i + \beta_0 e^{-\gamma r_{ij}^2}(x_j - x_i) + \alpha(rand - 0.5) \tag{10}$$

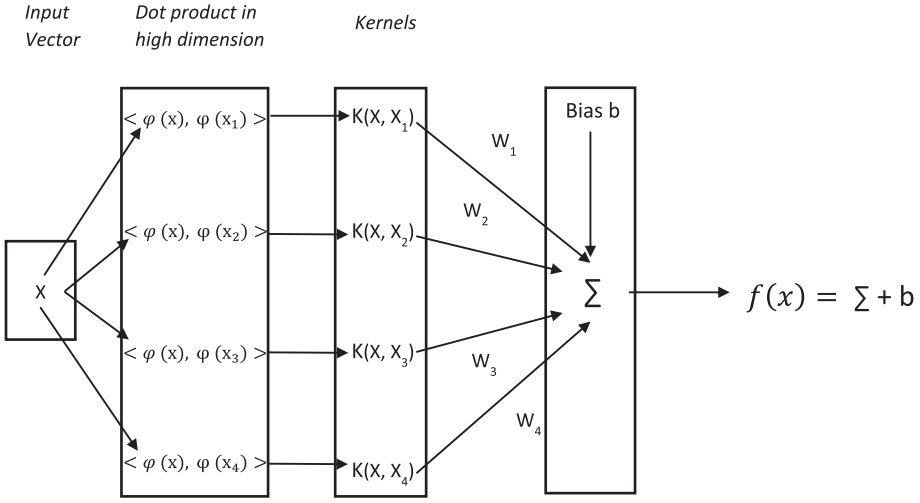

Fig. 2. Architecture of Support Vector Regression.

The second term is due to the attractiveness, whereas, the third term is based on the random movement of the firefly with randomization constant α. Rand is random number generator with values uniformly distributed between [0, 1]. Yang [27] recommended to gradually decrease α as the optima approaches to improve the quality of solution using Eq. (11).

$$delta = 1 - \left(\frac{10^{-4}}{0.9}\right)^{\frac{1}{NGen}}$$
$$\alpha\_new = (1 - delta) * \alpha; \quad (11)$$

where *NGen* is the new generation number, α_new is the reduced value of α, and *delta* is factor with which the randomization parameter is decreased.

4. Brief introduction on aggregate image measurement system

Aggregate Image Measurement System is an automated digital image processing technique that captures aggregate images at various resolutions and field of view with the help of different lighting schemes [29]. It is an integrated software consisting of camera, microscope, back-lighting and top-lighting systems, aggregate trays, along with a computer software to run the machine and analyze the data. It accurately measures aggregate shape parameters, namely, angularity, sphericity, and texture for coarse aggregates, while, angularity and form (2-D) for fine aggregates [19,29]. Angularity is a measure of sharpness of corner of a 2-dimensional image of aggregate. AIMS uses two methods for measurement of angularity, namely, gradient method and radius method. In the current study, radius method is used to measure the angularity of the aggregate. Radius method considers the difference between the particle radiuses in a certain direction with respect to an equivalent ellipse [19,20]. The equivalent ellipse has the same major and minor axes as the particle, but has no angularity. AIMS quantifies the particle as rounded, sub-rounded, sub-angular, angular, and highly angular. Texture is a measure of relative roughness or smoothness of the particle's surface. AIMS uses the wavelet method to measure aggregate texture and classifies the particle as polished, smooth, low, medium, and highly rough. The form indicates the change in the particle radius in all the directions and is measured by calculating the form index [20]. Three dimensions of a particle, i.e., longest dimension (d_l), intermediate dimension (d_i), and shortest dimension (d_s) are calculated for the sphericity measurements. Hence, texture is a micro level property of an aggregate, whereas, angularity, form, and sphericity represent the overall shape of a particle. Like angularity and texture, form and sphericity of a particle are also sub-divided into different groups. Detailed information about AIMS and shape characteristics can be found in previous literature [19,29].

5. Materials and experimental methodology

5.1. Material

A total of five loose asphalt mixes were collected from the production plant of Haskell Lemon Construction Company in Norman, Oklahoma. Four different types of mix samples were made out of each mix based on different level of target air voids (6, 8, 10 and 12%). The compacted samples were accepted when air voids was ±0.5%–1% of target air voids. The actual average air voids of three compacted sample at selected target air void reported in the Table 1. Thus, a total of 20 mixes (5 samples * 4 level of air voids) were prepared and were named M1 through M20. Table 1 show gradation and other properties of 20 mixes considered in the present study.

The levels of air voids were selected based on the assumption that they would cover the practical range of compaction densities of a pavement, i.e., 88–94% of maximum theoretical density. The collected mixes were prepared using three different types of aggregates, namely, limestone, rhyolite and granite. The mixes consisted of two different types of Superpave gradations with 19 and 12.5 mm nominal maximum size of aggregate (NMSA). Three different kinds of performance grade (PG) binders, namely, PG64-22, PG70-28, and PG76-28, were used to prepare the mixes. These binders were collected from the Valero Refinery in Ardmore, Oklahoma.

5.2. Sample preparation and E* testing

A Superpave gyratory compactor was used for preparation of the mixes with an aim to obtain the desired air-void content. Samples of sizes 100 mm diameter and 150 mm height were cut and cored from the initial 150 mm diameter and 167.5 mm height samples. Air void distribution was considered to be most consistent in these mixes in both horizontal and vertical directions [30]. A total 3 samples were compacted for each mix, leading to a total of 60 samples (3 samples * 20 mixes). Further, E* tests were conducted on these 60 samples in accordance with AASHTO TP62-06 [3]. A total of four temperatures (4, 21, 40, and 55 °C) and six frequencies (25, 10, 5, 1, 0.5, and 0.1 Hz) were considered for conducting the tests. A servo-hydraulic material testing system (MTS) was used for conducting the tests. Initially, the specimen were allowed to reach equilibrium within ±0.5 °C of the specified test temperature by placing it in the environmental chamber. Specimen deformation was measured using two LVDTs mounted on the specimen. Specimen was conditioned by applying 200 cycles of load at 25 Hz frequency prior to testing. Thus, a total of 1440 E* values were measured in the laboratory (20 mixes * 3 samples * 4 temperatures * 6 frequencies).

5.3. Measurement of aggregate shape parameters

After the E* testing was over, the aggregates from each samples were extracted using National Center for Asphalt Technology (NCAT) ignition oven. The aggregates of each mix were divided into following sizes of coarse aggregates: 19 mm–12.5 mm (P19-R12.5), 12.5 mm–9.5 mm (P12.5-R9.5), 9.5 mm–4.75 mm (P9.5-R4.75). Fine aggregates were divided into the following sizes: 4.75 mm–2.36 mm (P4.75-R2.36), 2.36 mm–1.18 mm (P2.36-R1.18). For the mixes compacted at different air void content, a slight difference in aggregate gradation was observed. The difference in gradation could be due to the fact that the samples with different air void content exert different pressure inside the compactor [31]. Also, the aggregates in the mix went through different laboratory processes, such as coring, compaction and sawing, which make it possible for the aggregate shape parameters to change or degrade. Further, retrieving aggregate from asphalt concrete will inevitably loose some fine aggregates. Consequently slight variation of aggregate gradation is pretty normal. Since, the aggregate gradation could not possibly explain the change in aggregate shape, the morphological properties of aggregates have to be measured separately. Aggregate shape parameters, namely, angularity, texture, sphericity and form, were measured using Pine's AIMS. AIMS was operated based on the guidelines and specifications laid by AASHTOTP81-10 [32].

5.3.1. Coarse aggregates

For each size of coarse aggregates, 2 samples comprising of 56 particles each were formed randomly. For coarse aggregates, the AIMS performs two scans for measurement of shape properties. For the first phase, only back-lighting is used to obtain a silhouette

Table 1
Aggregate gradation and properties of mixes.

Mix	Sieve Size(mm)											Avg. Air	Binder	Binder	Aggregate
	25	19	12.5	9.5	4.75	2.36	1.18	0.6	0.3	0.15	0.075				
	Percentage Passing (%)											Voids (%)	Type	(%)	Type
M1	100	97	90	85	72	48	33	24	16	9	6	5.5			
M2	100	98	90	86	74	50	34	25	17	9	6	7.2	PG 64-22	4.1	Limestone
M3	100	98	91	86	72	49	33	24	16	8	6	9.3			
M4	100	99	90	85	71	48	32	23	15	8	5	12.1			
M5	100	98	94	91	79	53	37	28	19	9	6	6.4			
M6	100	99	94	90	77	52	36	27	18	10	6	8.1	PG 76-28	4.1	Limestone
M7	100	99	91	87	75	49	34	26	17	9	5	9.9			
M8	100	99	92	87	76	50	35	26	17	8	5	12.0			
M9	100	100	97	91	70	49	36	27	16	7	4	6.2			
M10	100	100	98	91	71	50	37	27	16	7	4	8.0	PG 70-28	4.5	Granite
M11	100	100	98	93	74	52	38	28	17	7	4	10.3			
M12	100	100	98	91	73	52	37	27	16	7	4	12.1			
M13	100	100	96	90	76	52	38	29	20	10	7	6.1			
M14	100	100	96	91	76	52	38	29	20	10	7	8.1	PG 64-22	5.1	Rhyolite
M15	100	100	96	91	76	52	38	29	20	10	7	9.8			
M16	100	100	96	91	77	53	38	29	20	10	6	11.8			
M17	100	100	98	91	70	51	36	27	19	9	6	6.2			
M18	100	100	97	90	68	50	36	27	18	8	5	8.2	PG 76-28	4.2	Limestone
M19	100	100	97	89	67	48	35	26	18	8	5	9.5			
M20	100	100	98	90	69	50	36	26	18	8	5	12.1			

of the aggregate for angularity and form measurement. The second phase used top-lighting to quantify the aggregate texture and sphericity. Thus, a total of four shape measurements, angularity, texture, form and sphericity were obtained for each of 120 samples (20 mixes * 2 samples * 3 sizes), with each sample containing 56 particles.

5.3.2. Fine aggregates

The AIMS scan fine aggregates to obtain angularity and form measurements. Texture is not measured for fine aggregates as it was found to be highly correlated with the angularity [19]. Approximately, 50–100 g of fine aggregates consisting of 250–300 particles of each size were scanned using back-lighting. Initially, two samples of each sizes were tested. However, both samples showed similar values of angularity and form. Hence, it was decided to test only one sample for each size. Thus, angularity and form were measured for a total of 40 samples (20 mixes * 1 sample * 2 sizes) of fine aggregates.

5.3.3. Composite shape index factor

After the measurement of aggregate shape properties for all the sizes of coarse and fine aggregates a shape factors combining the effect of aggregate gradation with aggregate morphology were obtained. Pan et al. [33] used the same approach to quantify the effect of coarse aggregate morphology on the permanent deformation behavior of asphalt mix. Therefore, a composite shape index (CI) factor was calculated for each of the 20 mixes using

$$CI = \frac{\sum_{i=1}^{n}[(p_i)(s_i)]}{\sum_{i=1}^{n} p_i} \quad (12)$$

where n = total number of sieve sizes; p_i = % aggregate retained on a selected sieve, s_i = mean of shape parameter. The values of s_i (shape parameters) were measured using AIMS, which is not provided in this paper due to large volume of data. The further information can be obtained from elsewhere [36] (Values of p_i can be determined from Table 1. Thus, composite shape factors for angularity (CAI), texture (CTI), sphericity (CSI) and form (CFI) were calculated (refer Table 2).

6. Formulation of SVR-FA models

6.1. Database

The first and foremost step in prediction modeling is to set up the database consisting of independent and dependent variables. The original data set consisted of total 1440 E* values with independent variables, namely, cumulative shape index factors, volumetric properties of mixes, binder viscosity (η), and frequency (f) at which E* test were conducted. Log E* was considered as the dependent variable. Cumulative shape index factors included CAI, CFI, CTI and CSI as explained earlier. Volumetric properties of mix consisted of percentage air voids (V_a) and effective binder content (V_{beff}). Binder viscosity for each binder (PG64-22, PG70-28, and PG76-28) was calculated at the four test temperatures, i.e., 4, 21, 40, and 55 °C, according to the ASTM equation [34]. As per National Cooperative Highway Research Program [35], the values of slope and intercept for PG64-22, PG70-28 and PG76-28 are 10.98 and −3.68, 9.715 and −3.217, 9.2 and −3.024, respectively. Table 3 summarizes the descriptive statistics of each variable.

6.2. Division of database

The original database consisting of a total of 1440 data sets was divided into training and testing sets. Training set comprised of 1152 E* values (almost 80% of original data set), while testing set consisted of the remaining 288 E* values (about 20% of original data set). The separation of data into training and testing set was done randomly. The complete data set was standardized before use, i.e., each input variable was shifted to zero mean and unit standard deviation. Standardization is a very important step and enhances the accuracy of prediction [37].

6.3. Formulation of SVR-FA algorithm

All the computations in the present study were done using the commercial software MATLAB® installed on a personal computer with 8 GB RAM and Intel(R) core i7 @ 3.2 GHz processor. The gaussian radial basis kernel function (Eq. (13)) was used for non-linear mapping of the input data.

Table 2
Composite shape indices of mixes.

Mix Type	CAI	CFI	CTI	CSI
M1	10.564	7.314	144.041	0.696
M2	10.553	7.370	154.702	0.690
M3	10.769	7.420	153.357	0.684
M4	10.782	7.550	146.928	0.691
M5	10.530	7.330	138.762	0.687
M6	10.975	7.463	142.292	0.699
M7	10.767	7.432	142.360	0.689
M8	10.623	7.309	141.542	0.695
M9	10.719	7.574	235.134	0.690
M10	10.449	7.344	202.639	0.689
M11	10.530	7.226	211.912	0.718
M12	10.649	7.493	223.356	0.693
M13	10.769	7.533	147.442	0.691
M14	10.406	7.344	123.600	0.690
M15	10.692	7.381	149.413	0.710
M16	10.203	7.684	146.927	0.710
M17	10.808	7.465	141.772	0.761
M18	11.078	7.775	143.398	0.752
M19	10.404	7.299	140.801	0.707
M20	10.596	7.509	142.158	0.692

$$K(x_i, x_j) = \exp\left[-\frac{(x_i - x_j)^2}{2\sigma^2}\right] \quad (13)$$

where σ is the bandwidth of the gaussian radial basis function. The gaussian kernel tends to give good performance under general smoothness assumptions.

Initially, a grid search was performed to find the possible values of hyper-parameters, i.e., C, σ and ε. For fine tuning, the possible range consisting of these hyper-parameters was inputted to FA. The results of grid search and fine tuning through FA are shown in Table 4.

The hyper-parameters obtained were used to develop SVR-FA models. The developed SVR-FA models were used to predict the E^* for training and testing sets. The efficiency of these models were computed using performance evaluators such as, Mean Average Relative Error (MARE), Coefficient of Determination (R^2) and Overfitting Ratio (OR). The value of MARE should be as low as possible to indicate a good model performance. Value of R^2 and OR should approach 1. Higher R^2 implies higher correlation between predicted and measured values. OR represent the extent of generalizability of the model. If OR is close to 1, the model is likely to perform reliably on the unused data set. Table 5 shows the formulation for the performance evaluators used in this study.

7. Results and discussion

7.1. Results of SVR-FA algorithm

As explained earlier, SVR-FA models consisting of 8 independent variables, namely, V_a, V_{beff}, CAI CFI, CTI, CSI, η and f were developed. Figs. 3 and 4 depict the performance of SVR-FA model on training and testing sets, respectively. The results show that SVR-FA models successfully predict E^* with high correlation between measured and predicted data ($R^2 \approx 0.98$). The OR of the model is 1.17, which indicates that the model is almost free from overfitting.

Table 4
Values of hyper-parameters after grid search and FA.

	C	σ	ε
After grid search	1–10	10,000–100,000	0–1
After FA	4.041	68,605.193	0.023

Table 5
Performance evaluators.

Performance Evaluator	Formulation
Coefficient of Determination (R^2)	$\frac{\left[\sum_{k=1}^{n}(M_k - M_k^*).(P_k - P_k^*)\right]^2}{\sum_{k=1}^{n}(M_k - M_k^*).\sum_{k=1}^{n}(P_k - P_k^*)}$
Mean Absolute Average Error (MARE)	$\frac{\left[\sum_{k=1}^{n}(P_k - M_k)^2/P_k\right]}{n}$
Overfitting Ratio	$\frac{MARE_{test}}{MARE_{train}}$

Note: In these equations, M_k and P_k are the observed and predicted values, respectively. M_k^* and P_k^* are the mean of observed and predicted values, respectively.

7.2. Comparison between SVR-FA, ANN and SVR models

ANN model for E^* prediction were based on a feed-forward back-propagation algorithm having one input, two hidden and one output layer. The common Levenberg-Marquardt optimization algorithm was used for training the ANN model. Hyperbolic tangent and pure linear functions acted as activation functions for hidden and output layers, respectively. A detailed discussion about formulation of ANN models is given by Singh et al. [21]. The performance evaluators for SVR-FA, ANN and SVR are summarized in Table 6. ANN model shows minimum MARE value for both training and testing set as compared to both SVR-FA and SVR methods. However, overfitting ratio (OR) for ANN is much higher as compared to both SVR-FA and SVR algorithms that proves lack of generalization. Hence, SVR-FA and SVR models predict E^* with lesser accuracy but more reliability as compared to ANN. Figs. 5 and 6 depict the performance of ANN and SVR algorithms on testing set, respectively.

7.3. Formulation of SVR-FA model equations

As per Eq. (5), log E^* value can be predicted using the following equation

$$logE^* = \sum_{i=1}^{l}\left((\alpha_i - \alpha_i^*)\exp\left[-\frac{(x_i - x_j)^2}{2\sigma^2}\right] + b\right) \quad (14)$$

where $K(x_i, x_j)$ is the Gaussian kernel function as shown in Eq. (13), x_i is the set of support vectors and x_j is the input vector for which the E^* value is to be predicted. The values of Bias (b) and $(\alpha_i - \alpha_i^*)$ (non-zero for the support vectors) are obtained from MATLAB explicitly. Once the values of b, $(\alpha_i - \alpha_i^*)$ and σ are obtained, this equation may be effectively used by academicians and governmental agencies to predict the values of E^* with help of a simple spreadsheet, without in-depth knowledge about SVR-FA algorithm.

Table 3
Descriptive statistics of variables and correlation with E^*.

	V_a (%)	V_{beff} (%)	CAI	CFI	CTI	CSI	f (Hz)	η (10^5 Pa·s)	E^* (MPa)
Minimum	5.440	8.078	10.203	7.226	123.600	0.684	0.100	0.011	135
Mean	8.948	9.146	10.643	7.441	158.627	0.702	6.933	318.78	2864
Maximum	12.375	11.304	11.078	7.775	235.134	0.761	25.00	1805.42	18727
St. deviation	2.213	0.968	0.199	0.134	30.921	0.020	8.786	590.645	3262

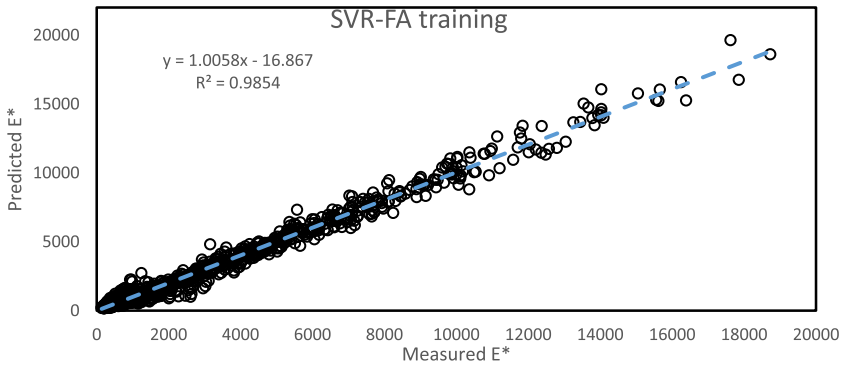

Fig. 3. Performance of SVR-FA on training set.

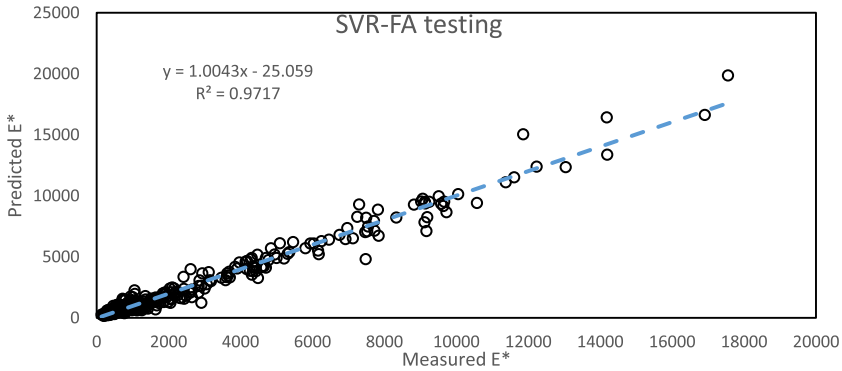

Fig. 4. Performance of SVR-FA on testing set.

Table 6
Performance of model on training and testing set.

Data Set	Performance Index	ANN	SVR-FA	SVR
Training	MARE (%)	10.2	20.67	23.12
	R^2	0.99	0.99	0.97
Testing	MARE (%)	17.5	24.12	26.13
	R^2	0.98	0.97	0.96
Complete	MARE (%)	11.7	21.3	24.29
	R^2	0.99	0.98	0.97
Overfitting ratio		1.72	1.17	1.13

7.4. Sensitivity analysis using SVR-FA models

The sensitivity of E^* was determined by developing SVR-FA models considering different combinations of input variables. Similar approaches to sensitivity analysis were used by Ceylan et al. [10] and Singh et al. [21] by developing ANN models. In the current study, 10 different combinations of input variables were considered. SVR-FA models were trained using 1152 E^* values (80% of the complete data) and tested using the remaining 288 E^* values (20% of complete data set). To judge the magnitude of sensitivity, R^2 and MARE of SVR-FA models were compared. The model with highest R^2 and lowest MARE tends to effect E^* the most.

Table 7 summarizes the statistics of different combinations of input variables. Although, SVR-FA models having CAI, CTI, CSI or CFI as their input variables, showed poor correlation ($R^2 = 0$), CSI model showed lesser MARE as compared to the other shape parameter models. V_a, V_{beff} and frequency models also showed poor correlation ($R^2 \approx 0$) with higher MARE (>120%). It is fact that asphalt mixes composed of aggregates and asphalt binder. Role of asphalt binder is to bind aggregate structure together and provide structural strength. Obviously aggregate parameters alone cannot pre-

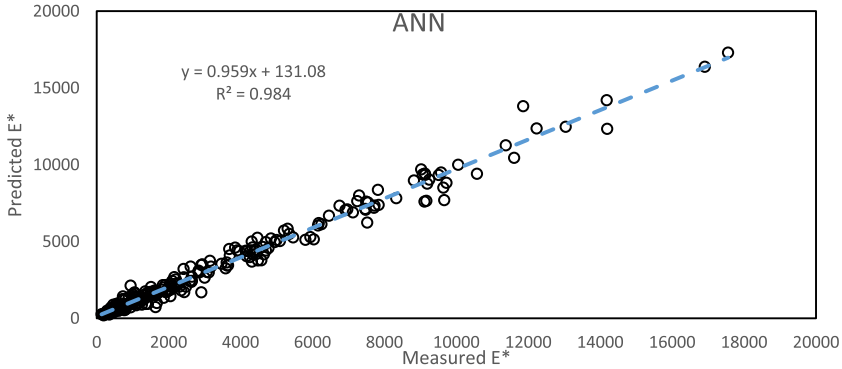

Fig. 5. Performance of ANN model on testing set.

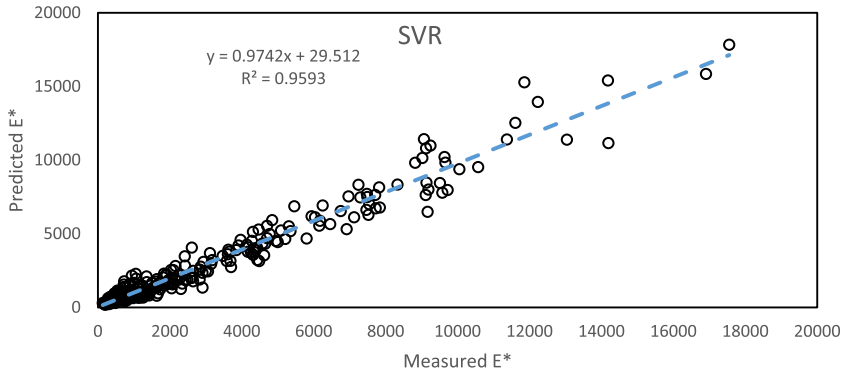

Fig. 6. Performance of SVR model on testing set.

Table 7
Sensitivity analysis of different combinations of input variables.

Combination #	Input Variables	R^2		MARE (%)	
		Training	Testing	Training	Testing
1	V_a	0.08	0.08	125.68	123.85
2	V_{beff}	0.00	0.01	132.96	130.85
3	CAI	0.00	0.00	136.17	134.23
4	CTI	0.00	0.00	137.46	134.95
5	CSI	0.01	0.01	118.16	115.34
6	CFI	0.00	0.00	130.52	129.01
7	f	0.06	0.06	124.11	122.40
8	η	0.56	0.56	76.91	75.73
9	f, η	0.72	0.72	63.43	62.72
10	V_a, V_{beff}, f, η	0.80	0.80	55.10	53.76

dict dynamic loading capacity of asphalt mixes, until unless we introduce rheological parameters of binder. Therefore, we did not see any correction among aggregate Viscosity model outperformed the models developed using other input variables by producing an R^2 = 0.56. SVR-FA models developed using a combination of η with f resulted in much better R^2 (=0.72) and lesser MARE (=63%). Finally, a combination of V_a, V_{beff}, η and f resulted in strongest correlation (R^2 = 0.80) and least error (MARE = 55%). Hence, a combination of η and f or V_a, V_{beff}, η and f could be used for E^* prediction with considerable accuracy. However, a combination of asphalt rheological properties, binder volumetric properties, loading frequency, aggregate gradations and shape parameters is required to produce optimum E^* prediction.

8. Conclusions

In the present study, SVR-FA approach was used for the prediction of E^* of asphalt mixes using the aggregate shape parameters, namely, angularity, sphericity, texture and form (2-D). The following conclusions were drawn from the study:

- SVR-FA is capable of successfully predicting the E^* values using shape parameters. The developed model predicted the E^* values of the complete data set with an R^2 of 0.98 and MARE of 21.36%.
- SVR-FA and SVR models showed better generalization capability as the overfitting ratio turned out to be very close to 1 as opposed to ANN. Though, the prediction accuracy was higher in case of ANN models.
- Asphalt rheology was found to be the most important factor for E^* prediction. Volumetric properties, composite shape factors and loading frequency cannot individually predict E^* with reasonable accuracy.
- Firefly algorithm proved instrumental in fine tuning the hyperparameters that resulted in the development of an efficient prediction model with lesser manual effort. This appeals for exploring the applications of evolutionary algorithms for civil engineering optimization problems.
- The approach discussed for formulation of model equations may be extensively used by the researchers and government agencies for E^* estimation without in-depth prior knowledge about the SVR-FA algorithm.

It is recommended that the database be increased to cover large variety of aggregates and mixes. This study is expected to be helpful for prediction of E^* using the aggregate shape parameters.

References

[1] S.W. Goh, Z. You, R.C. Williams, L. Xinjun, Preliminary E^* criteria of HMA for field rutting of asphalt pavements: Michigan's experience, J. Transp. Eng. 137 (1) (2011) 37–45.
[2] NCHRP, Guide for mechanistic-empirical design of new and rehabilitated pavement structures. Available one line at: http://trb.org/mepdg, National Cooperative Highway Research Program 1-37 A. Transportation Research Board, Washington, D.C, 2004.
[3] AASHTO, Standard method of test for determining dynamic modulus of hot-mix asphalt concrete mixtures. TP62-06, Standard Specifications for Transportation Materials and Methods of Sampling and Testing, 2005.
[4] J. Kim, T. Byron, G. Sholar, S. Kim, Development of E^* testing and data interpretation capability. Research Report FL/DOT/SMO/08-514, 2008.
[5] D. Andrei, M.W. Witczak, M.W. Mirza, Development of a Revised Predictive Model for the Dynamic (Complex) Modulus of Asphalt Mixtures. NCHRP 1-37A Interim Team Report, University of Maryland, College Park, 1999.
[6] J. Bari, M.W. Witczak, Development of a new revised version of the Witczak E^* predictive model for hot-mix asphalt mixtures, J. Assoc. Asphalt Paving Technol. 75 (2006) 381–423.
[7] G. Al-Khateeb, A. Shenoy, N. Gibson, T. Harman, A new simplistic model for E^* predictions of asphalt paving mixtures, J. Assoc. Asphalt Paving Technol. 75 (2006) 1254–1293.

[8] D.W. Christensen, T. Pellinen, R.F. Bonaquist, Hirsch model for estimating the modulus of asphalt concrete, J. Assoc. Asphalt Paving Technol. 72 (2003) 97–121.
[9] D.V. Singh, M. Zaman, S. Commuri, Evaluation of predictive models for estimating E* of HMA mixes used in Oklahoma. Transportation Research Record 2210, Transportation Research Board, 2011, pp. 57–72.
[10] H. Ceylan, K. Gopalakrishnan, S. Kim, Looking to the future: the next generation hot mix asphalt E* predictions models, Int. J. Pavement Eng. 10 (5) (2009) 341–352.
[11] H. Ceylan, C.W. Schwartz, S. Kim, K. Gopalakrishnan, Accuracy of predictive models for E* of hot-mix asphalt, J. Mater. Civ. Eng. 21 (6) (2009) 286–293.
[12] M.S.S. Far, B.S. Underwood, S.R. Ranjithan, Y.R. Kim, N. Jackson, Application of artificial neural networks for estimating E* of asphalt concrete. Transportation Research Record 2127, Transportation Research Board, Washington, DC, 2009, 173–186.
[13] H. Ceylan, K. Gopalakrishnan, S. Kim, Advanced approaches to hot-mix asphalt E* prediction, Can. J. Civ. Eng. 35 (7) (2008) 699–707.
[14] K. Gopalakrishnan, S. Kim, Support vector machines approach to HMA stiffness prediction, ASCE J. Eng. Mech. 137 (2) (2010) 138–146.
[15] K. Gopalakrishnan, S. Kim, H. Ceylan, Hot mix asphalt E* prediction using kernel machines, ANNIE, ANNs in Engineering, St. Lou is, Missouri, November 2–4, 2009, pp.131–138.
[16] Y.B. Dibike, S. Velickov, D. Solomatine, M.B. Abbott, Model induction with support vector machines: introduction and applications, J. Comput. Civil Eng. 15 (3) (2001) 208–216.
[17] M. Soltani, T. Moghaddam, M. Karim, S. Shamshirb, C. Sudheer, Stiffness performance of polyethylene terephthalate modified asphalt mixtures estimation using support vector machine-firefly algorithm, Elsevier Meas. 63 (2015) 232–239.
[18] T. Moghaddam, M. Soltani, H. Shahraki, S. Shamshirband, N. Noor, M. Karim, The use of SVM-FFA in estimating fatigue life of polyethylene terephthalate modified asphalt mixtures, Elsevier Meas. 90 (2016) 526–533.
[19] E. Masad, T. Al-Rousan, M. Bathina, J. McGahan, C. Spiegelman, Analysis of aggregate shape characteristics and its relationship to HMA performance, Road Mater. Pavement Des. 8 (2) (2007) 317–350.
[20] E. Masad, D. Olcott, T. White, L. Tashman, Correlation of fine aggregate imaging shape indices with asphalt mixture performance. Transportation Research Record 1757, Transportation Research Board, Washington, DC, 2001, 148–156.
[21] D. Singh, M. Zaman, S. Commuri, Artificial neural network modeling for E* of hot mix asphalt using aggregate shape properties, J. Mater. Civil Eng. 25 (1) (2012) 54–62.
[22] D. Singh, M. Zaman, S. Commuri, Inclusion of aggregate angularity, texture, and form in estimating E* of asphalt mixes, Road Mater. Pavement Des. 13 (2) (2012) 327–344.
[23] V. Vapnik, Statistical Learning Theory, Wiley, New York, USA, 1998, p. 736.
[24] V. Vapnik, The Nature of Statistical Learning Theory, Springer, NY, USA, 1995, p. 314.
[25] E. Alpaydin, Introduction to Machine Learning, The MIT Press Google Scholar, Cambridge, Massachusettes, 2004.
[26] A. Smola, B. Scholkopf, A tutorial on support vector regression, Stat. Comput. 14 (2004) 199–222.
[27] X. Yang, Firefly Algorithms for Multimodal Optimization. International Symposium on Stochastic Algorithms, Springer Berlin Heidelberg, 2009, pp. 169–178.
[28] J. Olamaei, M. Moradi, T. Kaboodi, A new adaptive modified firefly algorithm to solve optimal capacitor placement problem, in: Proceedings of the 18th Conference on Electrical Power Distribution Networks (EPDC), Kermanshah, Iran, 2013, pp. 1–6.
[29] E.A. Masad, Aggregate imaging system (AIMS) basics and applications. Rep. No. FHWA/TX-05/5-1707-01-1, Texas Transportation Institute, Texas A&M Univ. System, College Station, TX, 2005.
[30] G.R. Chehab, Characterization of asphalt concrete in tension using a visco-elasto-plastic model (Ph.D. dissertation), North Carolina State Univ., Raleigh, NC, 2002.
[31] E. Mahmoud, E. Masad, Experimental methods for the evaluation of aggregate resistance to polishing, abrasion, and breakage, ASCE J. Mater. Civil Eng. 19 (2011) 977–985. MTS System Corporation. Retrieved from July 12, 2011, http://www.mts.com/.
[32] AASHTO, Determining aggregate shape properties by means of digital image analysis, TP81-10, Washington, DC, 2010.
[33] T. Pan, E. Tutumluer, S.H. Carpenter, Effect of coarse aggregate morphology on permanent deformation behavior of hot mix asphalt, J. Transp. Eng. 132 (7) (2006) 580–589.
[34] ASTM, Viscosity-temperature chart for asphalt, Annual book of ASTM standards, Vol. 0.0403, D2493, West Conshohocken, PA, 2009.
[35] National Cooperative Highway Research Program (NCHRP), Development of the 2002 guide for the design of new and rehabilitated pavement structures. 1-37 A, Phase II, Transportation Research Board, Washington, DC, 2004.
[36] D.V. Singh, A Laboratory Investigation and Modeling of Dynamic Modulus of Asphalt Mixes for Pavement Applications. ProQuest Publication, USA, 2011, 317. ISBN No. 978-1-2670-4598-0.
[37] S. Ghosh, P. Mujumdar, Statistical downscaling of GCM simulations to streamflow using relevance vector machine, Elsevier Adv. Water Resour. 31 (1) (2007) 132–146.